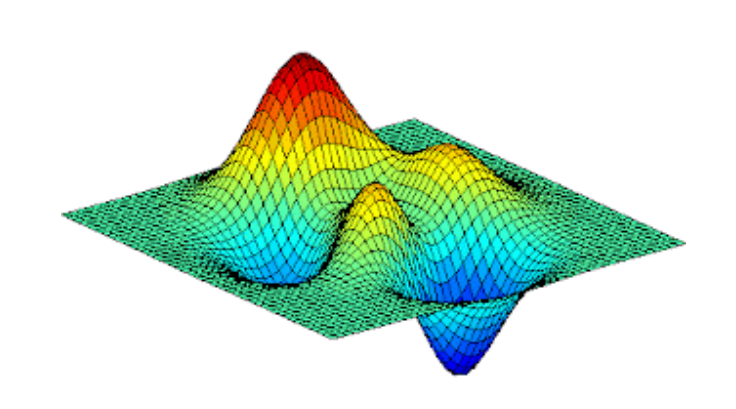


Realizing Negative Quantum States with the IBM Quantum Hardware





Jai Lalita

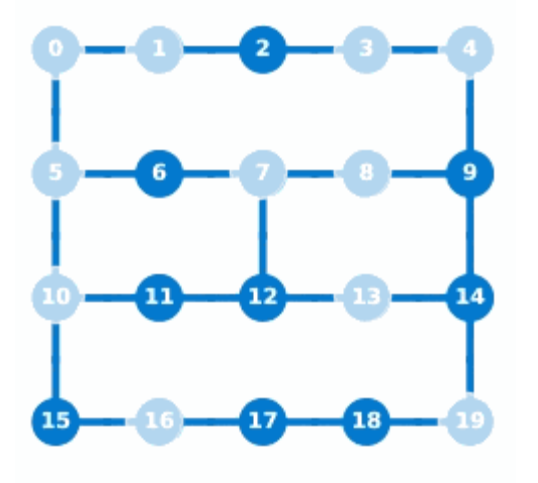
pursuing Ph.D. under the guidance of

Prof. Subhashish Banerjee

at

Department of Physics

Indian Institute of Technology Jodhpur, India - 342030



- 1. **J. Lalita**, K.G. Paulson, and S. Banerjee, Annalen der Physik **535**, 2300139 (2023).
- 2. **J. Lalita** and S. Banerjee, *Phys. Scr.* **99**, 035116 (2024).
- 3. J. Lalita, P.S. Iyer, and Subhashish Banerjee, arXiv:2411.04608 (2024).

Brief history and motivation:



➤ Wigner formalism, i.e., phase space formalism

JUNE 1, 1932

PHYSICAL REVIEW

VOLUME 40

On the Quantum Correction For Thermodynamic Equilibrium

By E. WIGNER

Department of Physics, Princeton University

(Received March 14, 1932)

The probability of a configuration is given in classical theory by the Boltzmann formula $\exp\left[-V/hT\right]$ where V is the potential energy of this configuration. For high temperatures this of course also holds in quantum theory. For lower temperatures, however, a correction term has to be introduced, which can be developed into a power series of h. The formula is developed for this correction by means of a probability function and the result discussed.



E. Wigner

Awarded Nobel Prize in 1963.

Discrete Wigner function formalism, i.e., Gibbons et. al. formalism

PHYSICAL REVIEW A 70, 062101 (2004)

Discrete phase space based on finite fields

Kathleen S. Gibbons, ^{1,2} Matthew J. Hoffman, ^{1,3} and William K. Wootters ¹ Department of Physics, Williams College, Williamstown, Massachusetts 01267, USA ² Department of Theology, University of Notre Dame, Notre Dame, Indiana 46617, USA ³ Department of Mathematics, University of Maryland, College Park, Maryland 20742, USA (Received 25 May 2004; published 3 December 2004)



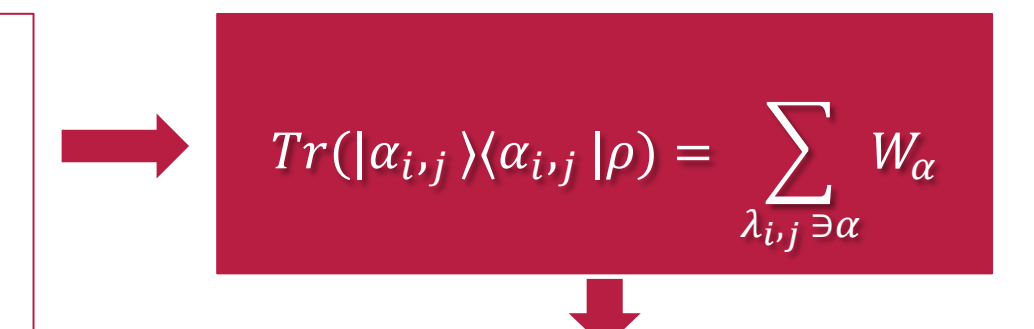
W.-K. Wootters

What are negative quantum states?



Are a normalized set of real numbers distributed over a two-dimensional grid of points.

- To define discrete Wigner functions we need to choose two one-to-one maps:
 - (1). Each basis set B_i is associated with each striation S_i and
 - (2). Each basis vector $|\alpha_{i,j}\rangle$ is associated with a line $\lambda_{i,j}$.



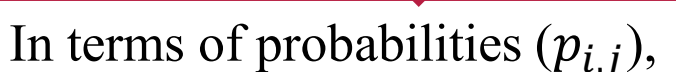


Negative quantum states are the normalized eigenvector corresponding to the negative eigenvalues of $A(\alpha)$. The state corresponding to the normalized eigenvector of most negative eigenvalue of $A(\alpha)$ is $|NS_1\rangle$. Analogously, the second and third negative quantum states are represented by $|NS_2\rangle$ state and $|NS_3\rangle$ state, corresponding to the normalized eigenvectors of second and third most negative eigenvalues of $A(\alpha)$, respectively, and so on.

In terms of phase point operator $A(\alpha)$,

$$W_{\alpha} = \frac{1}{d} \left(Tr \left[\rho \, A(\alpha) \right] \right)$$

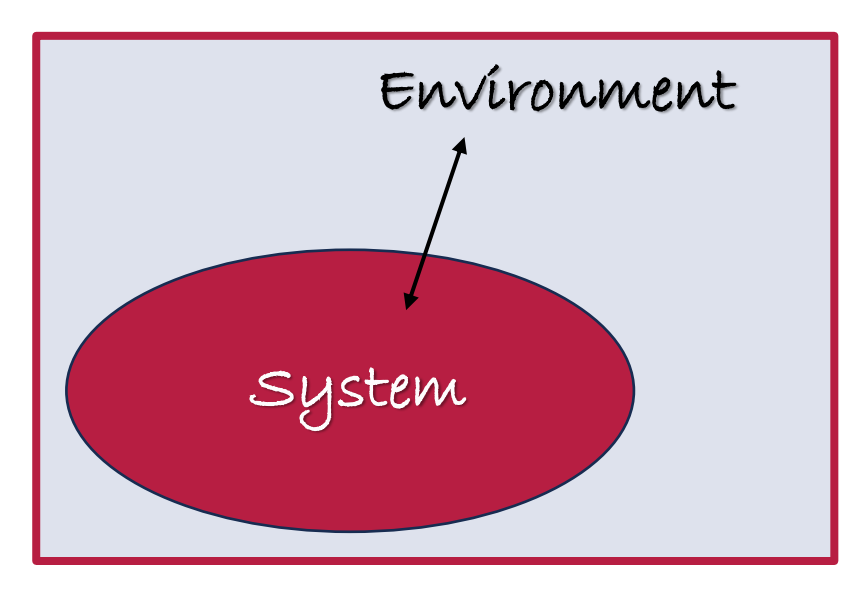
here,
$$\mathbf{A}(\boldsymbol{\alpha}) = \sum_{\lambda_{i,j} \ni \alpha} \mathbf{P}_{i,j} - 1$$
, and $\mathbf{P}_{i,j} = |\alpha_{i,j}\rangle\langle\alpha_{i,j}|$.



$$W_{\alpha} = \frac{1}{d} \left(\sum_{\lambda_{i,j} \ni \alpha} p_{i,j} - 1 \right)$$

What is their importance?





Open quantum system

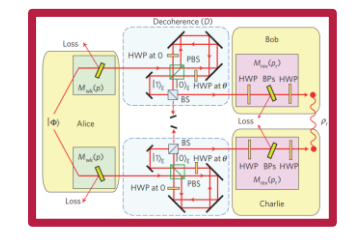
- Noise emerges as an artefact of the system's interaction with its ambient environment.
- \triangleright Mathematical formalism for the operation of noisy channels on ρ is

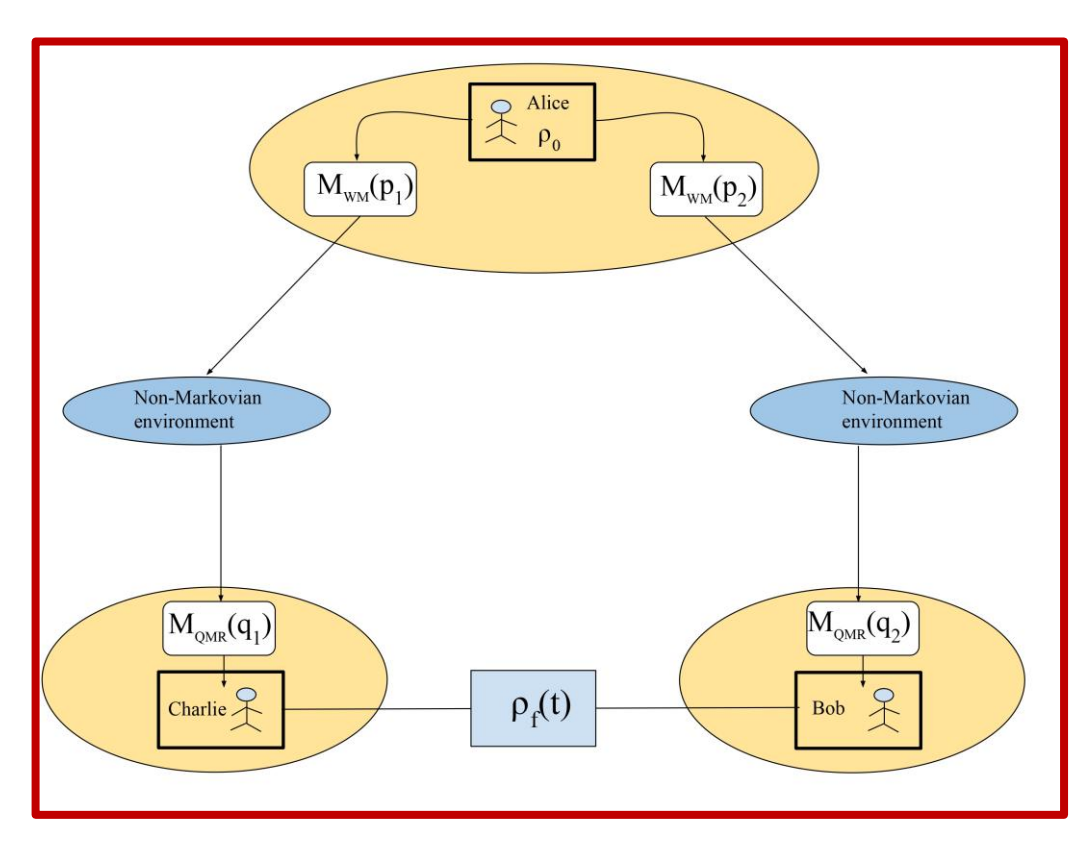
$$\rho(t) = \sum_{i} K_i(t) \rho(0) K_i^{\dagger}(t),$$

here K_i 's are the Kraus operators, characterizing the noise.

- Depending on the noise, system's dynamics can be Markovian (memoryless) or non-Markovian (information backflow).
- ➤ We have particularly considered the (non)-Markovian unital, (random telegraph noise (RTN)) and non-unital (amplitude damping (AD)) noisy channels.

Physical Model WM and QMR:





Schematic diagram for protecting quantum correlations of negative quantum states and Bell state using weak measurement (M_{WM}) and quantum measurement reversal (M_{OMR}).

Alice first performs weak measurement $(M_{WM}(p_1, p_2))$, on the negative quantum states before distribution to Bob and Charlie via non-Markovian noisy quantum channels.

$$M_{WM}(p_1, p_2) = \begin{pmatrix} 1 & 0 \\ 0 & \sqrt{1 - p_1} \end{pmatrix} \otimes \begin{pmatrix} 1 & 0 \\ 0 & \sqrt{1 - p_2} \end{pmatrix}$$

Bob and Charlie perform quantum measurement reversal $(M_{QMR}(q_1, q_2))$, on receiving the qubits.

$$M_{QMR}(q_1, q_2) = \begin{pmatrix} \sqrt{1 - q_1} & 0 \\ 0 & 1 \end{pmatrix} \otimes \begin{pmatrix} \sqrt{1 - q_2} & 0 \\ 0 & 1 \end{pmatrix}$$

The resulting state $\rho_f(t)$, can be made maximally entangled by choosing appropriate (p1, p2) and (q1, q2). Further, the state $\rho_f(t)$ can also be used for quantum teleportation (QT) between Bob and Charlie.

$$\rho_f(t) = \frac{M_{QMR}\left(\sum_{i=0}^1 \sum_{j=0}^1 K_{ij} \left[M_{WM} \rho(0) M_{WM}^{\dagger}\right] K_{ij}^{\dagger}\right) M_{QMR}^{\dagger}}{P^{succ}},$$

here, $K_{ij} = K_i \otimes K_j$ are the Kraus operators of the non-Markovian noise and,

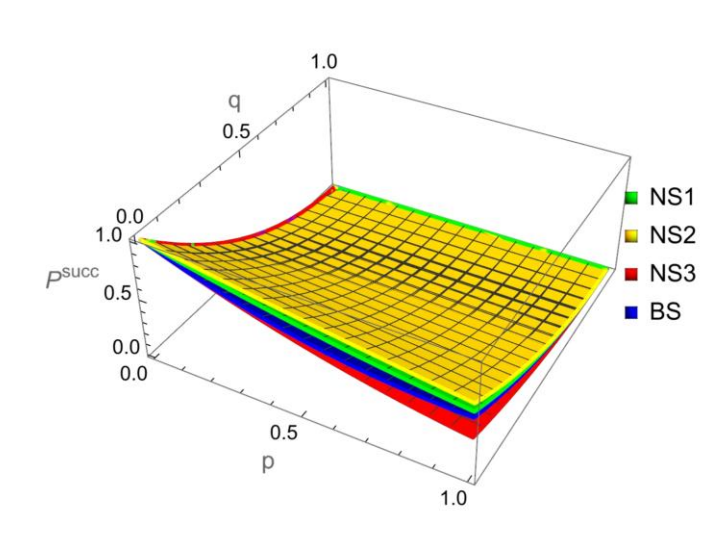
$$P^{succ} = Tr \big[M_{QMR} \big(\sum_{i=0}^{1} \sum_{j=0}^{1} K_{ij} \big[M_{WM} \, \rho(0) M_{WM}^{\dagger} \big] \, K_{ij}^{\dagger} \big) M_{QMR}^{\dagger} \big].$$

Results: Quantum correlations and UQT requirements



Quantum correlations and UQT requirements	Without WM and QMR	With WM and QMR
Concurrence	$ NS_3\rangle > \phi^+\rangle > NS_1\rangle > NS_2\rangle$	$ NS_2\rangle > NS_1\rangle > NS_3\rangle > \phi^+\rangle$
Discord	$ NS_3\rangle = \phi^+\rangle > NS_1\rangle > NS_2\rangle$	$ NS_2\rangle > NS_1\rangle \approx \phi^+\rangle > NS_3\rangle$
Two (three)- measurement steering	$ \phi^+\rangle > NS_3\rangle > NS_1\rangle > NS_2\rangle$	$ NS_2\rangle > NS_1\rangle > \phi^+\rangle > NS_3\rangle$
Maximal Fidelity	$ \phi^+\rangle > NS_3\rangle > NS_1\rangle > NS_2\rangle$	$ NS_2\rangle > NS_1\rangle > \phi^+\rangle > NS_3\rangle$
Fidelity deviation	$ NS_3\rangle < \phi^+\rangle < NS_1\rangle < NS_2\rangle$	$ NS_2\rangle \approx NS_1\rangle < NS_3\rangle < \phi^+\rangle$

TABLE I. Comparison of the quantum correlations, maximal fidelity, and fidelity deviation variations of two-qubit $|NS_1\rangle(p=0.17, q=0.54), |NS_2\rangle(p=0.05, q=0.74), |NS_3\rangle(p=0.05, q=0.05),$ and the Bell $|\phi^+\rangle$ state (p=0.01, q=0.01) under the non-Markovian AD channel (t>0).

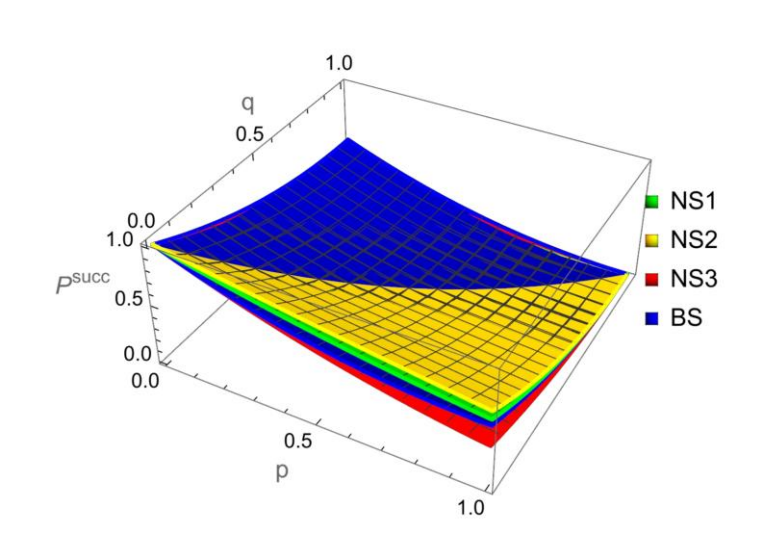


Variation of success probability of the NS_1 , NS_2 , NS_3 and Bell state under non-Markovian AD channel with WM strength (p), and QMR strength (q) at time t=10.

Results: Quantum correlations and UQT requirements



Quantum correlations and UQT requirements	Without WM and QMR	With WM and QMR
Concurrence	$ NS_3\rangle \approx \phi^+\rangle > NS_1\rangle > NS_2\rangle$	$ NS_2\rangle \approx NS_3\rangle \approx \phi^+\rangle > NS_1\rangle$
Discord	$ NS_3\rangle > \phi^+\rangle > NS_1\rangle > NS_2\rangle$	$ NS_2\rangle > NS_3\rangle > \phi^+\rangle > NS_1\rangle$
Two (three)- measurement steering	$ \phi^+\rangle > NS_3\rangle > NS_1\rangle > NS_2\rangle$	$ \phi^+\rangle > NS_2\rangle \approx NS_3\rangle > NS_1\rangle$
Maximal Fidelity	$ \phi^+\rangle > NS_3\rangle > NS_1\rangle > NS_2\rangle$	$ \phi^+\rangle > NS_2\rangle \approx NS_3\rangle > NS_1\rangle$
Fidelity deviation	$ NS_3\rangle < NS_1\rangle < NS_2\rangle < \phi^+\rangle$	$ NS_2\rangle = 0 < NS_3\rangle < NS_1\rangle < \phi^+\rangle$



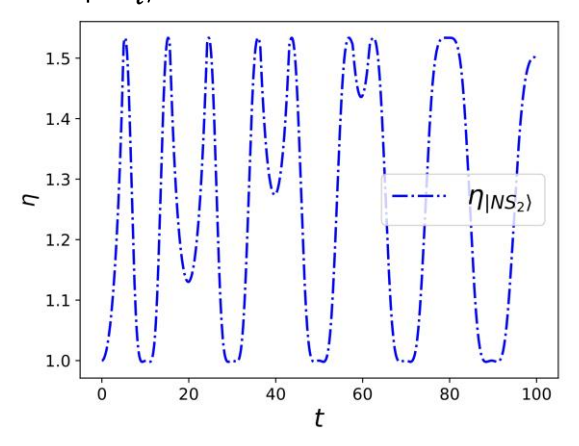
Variation of success probability of the NS_1 , NS_2 , NS_3 and Bell state under non-Markovian RTN channel for WM strength (p), and QMR strength (q) at time t = 10.

TABLE II. Comparison of the quantum correlations, maximal fidelity, and fidelity deviation variations of two-qubit $|NS_1\rangle$ (p=0.17, q=0.54), $|NS_2\rangle$ (p=0.05, q=0.74), $|NS_3\rangle$ (p=0.05, q=0.05), and the Bell $|\phi^+\rangle$ state (p=0.01, q=0.01) under the non-Markovian RTN channel (t>0).

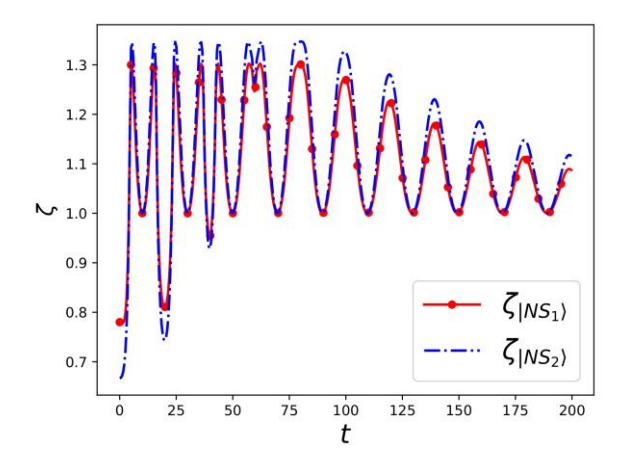
Results: Maximal CHSH violation and Maximal mean quantum Fisher information (QFI)



(i) : $\eta_{|NS_i\rangle}$ under non-Markovian AD



(ii) : $\zeta_{|NS_i\rangle}$ under non-Markovian AD



- Here $\eta_{|NS_i\rangle}$ denotes the ratio of maximal CHSH violation (S_{max}) for $|NS_i\rangle$ state to that of the Bell $|\phi^+\rangle$ state with WM and QMR.
- With the WM and QMR, the $|NS_2\rangle$ state shows more frequent revivals above the classical limit 2, which means it retains non-locality better, while the Bell $|\phi^+\rangle$ state often stays below 2 under non-Markovian AD noise.

- ightharpoonup Here $\zeta_{|NS_i\rangle}$ denotes the ratio of maximal mean QFI for $|NS_i\rangle$ state to that of the Bell $|\phi^+\rangle$ state.
- The $|NS_1\rangle$ and $|NS_2\rangle$ states maintain a higher maximal mean QFI for longer duration in comparison to the Bell $|\phi^+\rangle$ state making them better suited for realistic quantum metrology applications under noise.

How can we realize these states physically?



Gram-Schmidt procedure

- Step 1 : Consider any two-qubit negative quantum states, i.e., either of the $|NS_1\rangle$, $|NS_2\rangle$, $|NS_3\rangle$, and $|NS_3'\rangle$ as $|V_1\rangle$. Let $|V_1\rangle = |NS_1\rangle$.
- Step 2 : To find the other three orthonormal vectors $(|V_2\rangle, |V_3\rangle, |V_4\rangle)$ of $|V_1\rangle$, we take any three linearly independent vectors of $|V_1\rangle$. We pick the standard computational basis vectors $|e_1\rangle = |00\rangle$, $|e_2\rangle = |01\rangle, |e_3\rangle = |10\rangle$ as linearly independent vectors of $|V_1\rangle$. Considering $|O_2\rangle = |e_1\rangle$, $|O_3\rangle = |e_2\rangle, |O_4\rangle = |e_3\rangle$, the orthonormal vectors $|V_2\rangle, |V_3\rangle$, and $|V_4\rangle$ can be calculated using the Gram-Schmidt decomposition as

$$|V_{K+1}\rangle = \frac{|O_{K+1}\rangle - \sum_{i=1}^{k} \langle V_i | O_{K+1} \rangle |V_i\rangle}{\left| \left| |O_{K+1}\rangle - \sum_{i=1}^{k} \langle V_i | O_{K+1} \rangle |V_i\rangle \right|\right|}$$

- Step 3: Now, we have four orthonormal vectors $|V_1\rangle$, $|V_2\rangle$, $|V_3\rangle$, and $|V_4\rangle$, which can span the two-qubit system's Hilbert space.
- Step 4: Finally, the unitary transformation U from the computational basis set $\{|e_i\rangle\}$ to the orthonormal set $\{|V_i\rangle\}$ is given by $U = \sum_{i=1}^4 |V_i\rangle \langle e_i|$, which takes the vector $|00\rangle$ to the state $|NS_1\rangle$.

Corresponding quantum circuits:



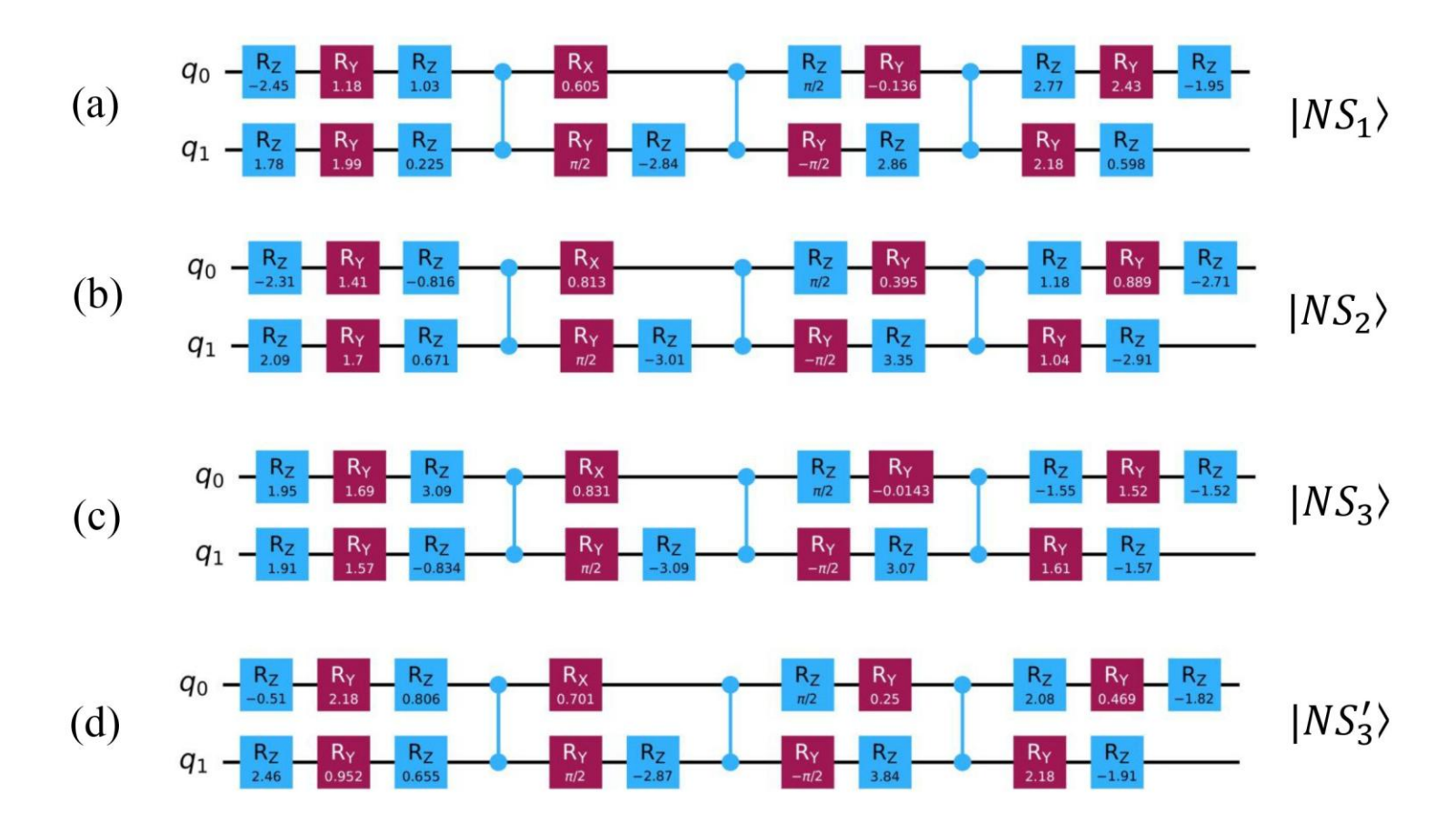


FIG. 1: Quantum circuits to generate the two-qubit $|NS_1\rangle$, $|NS_2\rangle$, $|NS_3\rangle$, and $|NS_3'\rangle$ states from the $|00\rangle$ state using H, R_x , R_z , and CZ gates are shown in subfigures (a), (b), (c), and (d) respectively. Here, q_0 and q_1 represent the qubits in the $|00\rangle$ state.

Results: State Tomography



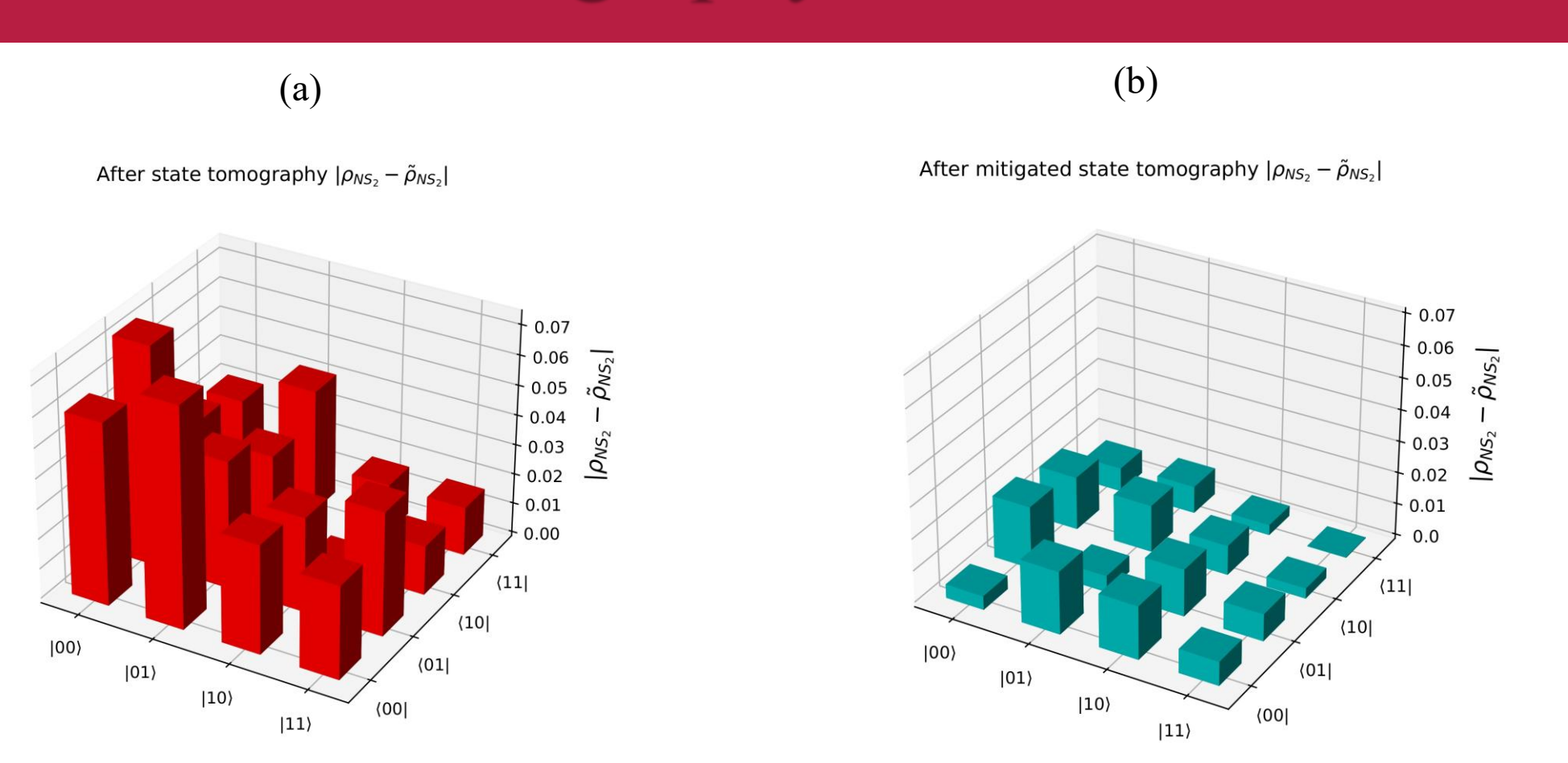


Fig 2: The city plot for the $|NS_2\rangle$ state displays the absolute difference between the components of the original $|NS_2\rangle$ state and the $|NS_2\rangle$ state obtained after performing a mitigated state tomography experiment on the real IBM quantum computer *ibm_brisbane* for 8192 times.

Results: State Tomography

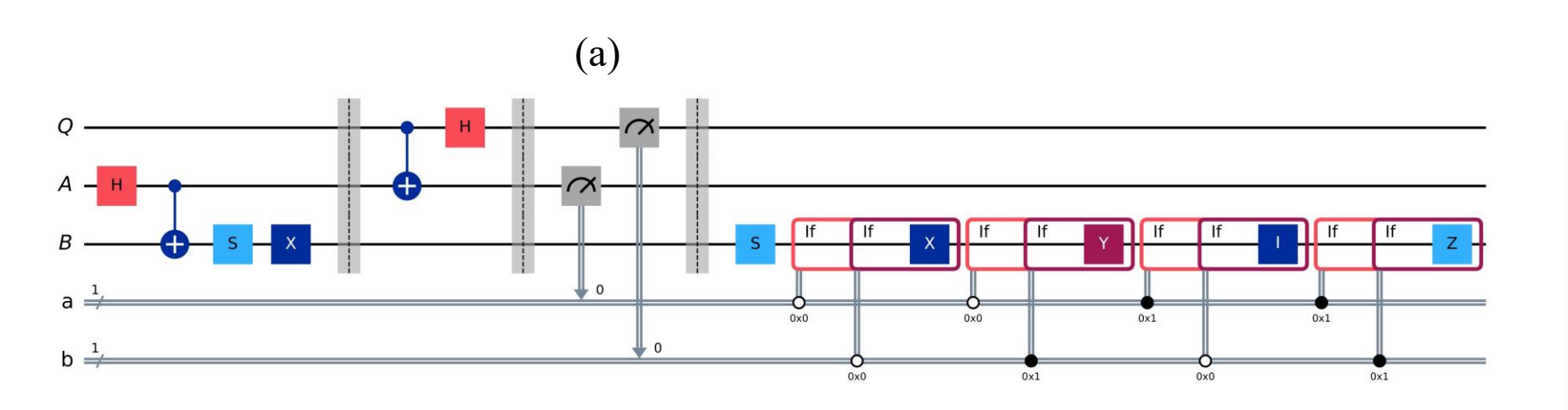


Negative	Circuit	Circuit	Schmidt	Fidelity			
Quantum States	depth	complexity	Rank	StateTomography		MitigatedStateTomography	
				On simulator	On IBM quantum	On simulator	On IBM quantum
					computer		computer
					(ibm_brisbane)		(ibm_brisbane)
$ NS_1\rangle$	13	3	2	0.92	0.87 ± 0.01	0.97	0.99 ± 0.01
$ NS_2\rangle$	13	3	2	0.93	0.88 ± 0.01	0.97	0.98 ± 0.01
$ NS_3\rangle$	13	3	2	0.91	0.89 ± 0.01	0.97	0.98 ± 0.01
$ NS_3'\rangle$	13	3	2	0.91	0.89 ± 0.01	0.96	0.98 ± 0.01
$ NS_3''\rangle$	4	1	2	0.93	0.91 ± 0.01	0.99	0.99 ± 0.01
Bell state $(\phi^+\rangle)$	2	2	2	0.93	0.90 ± 0.01	0.99	0.99 ± 0.01

TABLE I: Comparison of circuit depth, complexity, Schmidt rank, and fidelity after performing state tomography and mitigated state tomography on IBM *AerSimulator* and real quantum computer *ibm_brisbane* of the negative quantum states and the Bell state ($|\phi^+\rangle$).

Results: Teleportation using $|NS_3''\rangle$ state





ab	Operation on B	Final State of B
00	SX	$\alpha 0\rangle + \beta 1\rangle$
01	SY	$\alpha 0\rangle + \beta 1\rangle$
10	SI	$\alpha 0\rangle + \beta 1\rangle$
11	SZ	$\alpha 0\rangle + \beta 1\rangle$

(b)

FIG. 3: (a) Circuit for implementing quantum teleportation scheme using $|NS_3''\rangle$ as an entangled resource. The quantum gates in the blocks annotated with "if" are applied conditioned on the values of the classical bits corresponding to the measurement outcomes.

(b) Alice transmits the classical information (ab) to Bob through a classical communication channel. Based on the received classical bits, Bob performs specific unitary operations on his qubit (denoted as operation on B). Following the application of these operations, the resulting final state of Bob's qubit(Final state of B) corresponds precisely to the unknown quantum information originally intended for teleportation.

Results: Fidelity



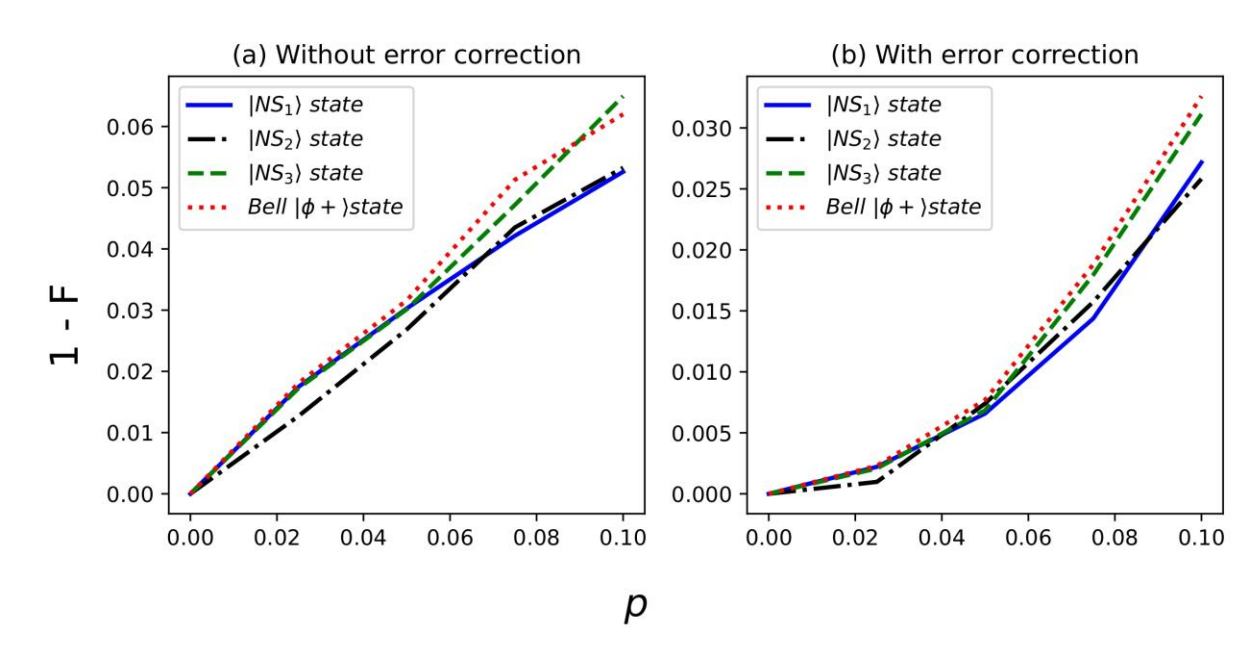


FIG. 4: Variation of (1 - F) for $|NS_1\rangle$, $|NS_2\rangle$, $|NS_3\rangle$, and $|\phi^+\rangle$ Bell state with depolarizing error probability p (a) without any error correction and (b) after implementing Shor's error correction.

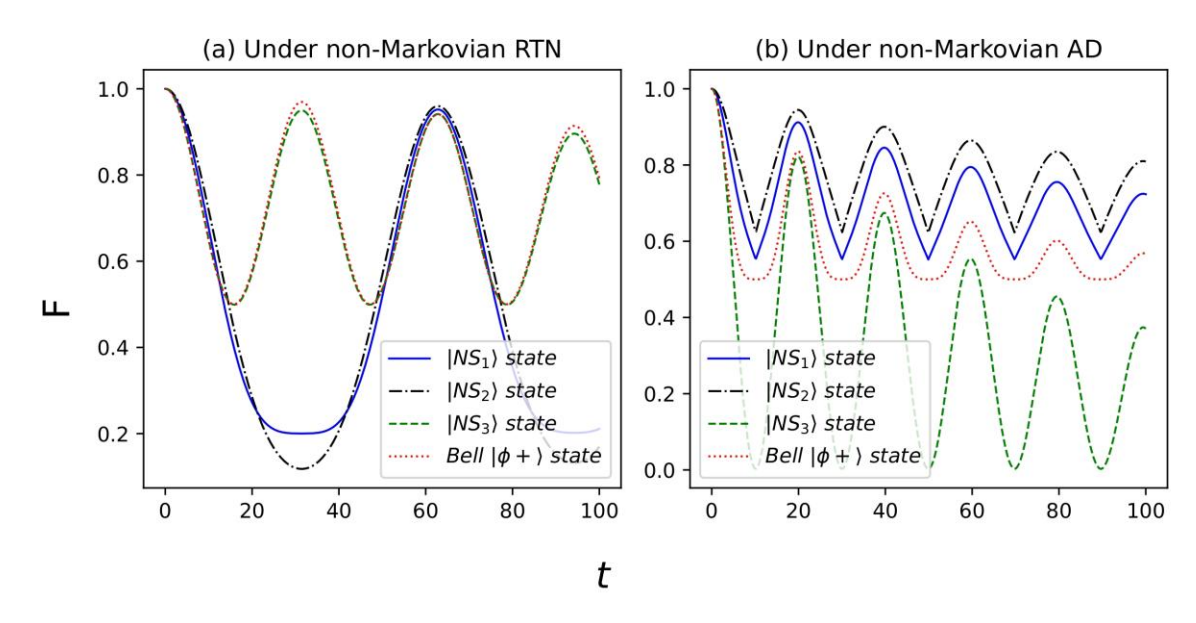


FIG. 5: Variation of fidelity of $|NS_1\rangle$, $|NS_2\rangle$, $|NS_3\rangle$, and $|\phi^+\rangle$ Bell state with time (a) under non-Markovian RTN for b=0.05 and $\gamma^{RTN}=0.001$, (b) under non-Markovian AD for g=0.01 and $\gamma^{AD}=5$.

Conclusion:



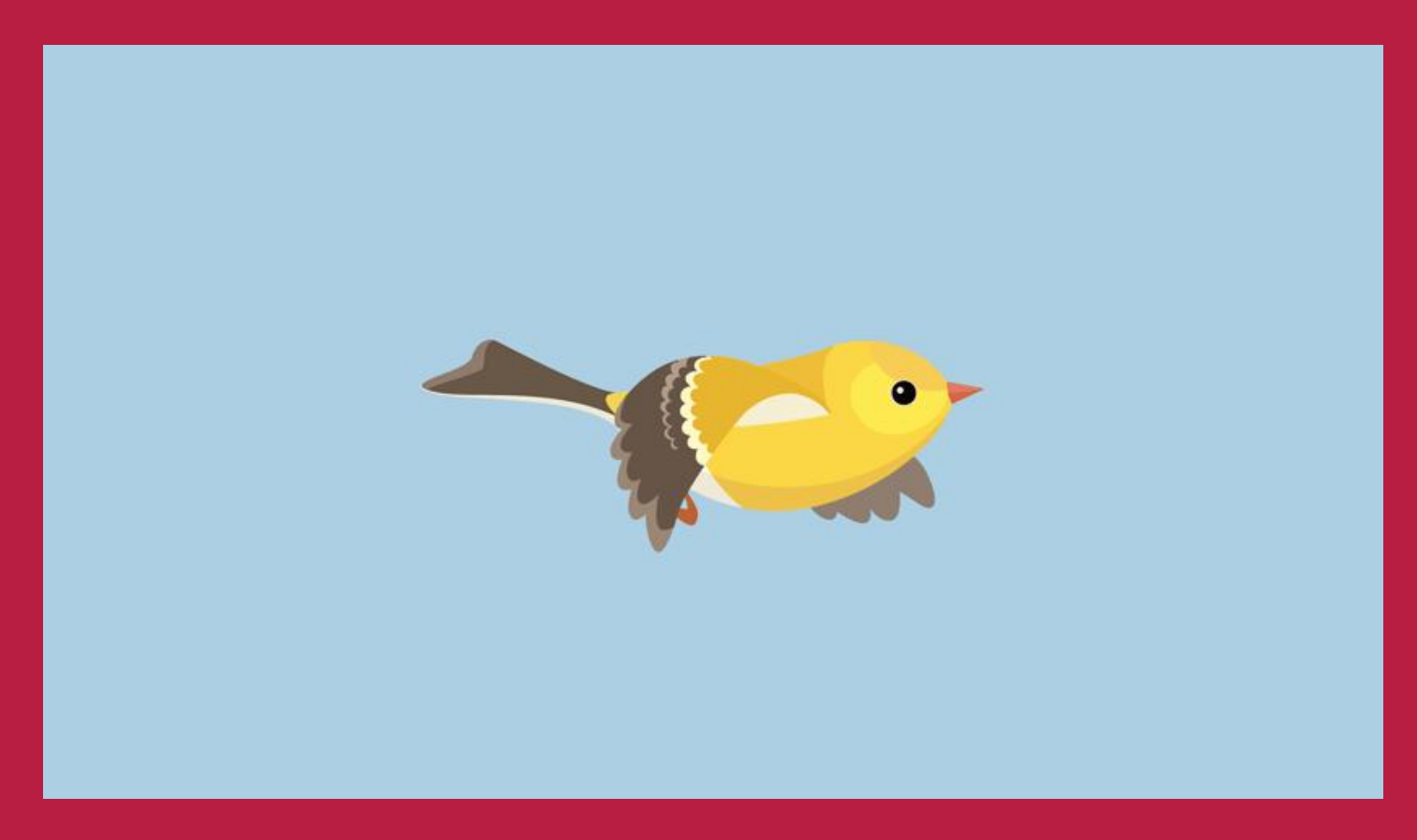
- This study introduces innovative methods for generating stable entangled two-qubit negative quantum states, supported by detailed quantum circuit designs for practical implementations.
- We demonstrated high-fidelity results for these states in simulated environments and on real quantum hardware through quantum state tomography and mitigation techniques.
- The high fidelity of these states, even under non-Markovian noise, underscores their utility in quantum teleportation and other applications requiring robust entanglement.
- Extending these methodologies to multi-qubit systems holds promise for creating durable quantum memories, essential for long-term quantum information storage and processing.
- **J. Lalita** and S. Banerjee, "A two-qubit collision model: non-Markovianity and non-classicality." (https://arxiv.org/abs/2506.23818)
- ▶ **J. Lalita** and S. Banerjee, "Interrelation of Non-Classicality, Entropy, Irreversibility and Work extraction in Open Quantum Systems." (https://arxiv.org/abs/2510.15140)

References



- 1. Banerjee, S. Open Quantum Systems: Dynamics of Nonclassical Evolution (Springer, Singapore 2018).
- 2. H. -P. Breuer, F. Petruccione, The Theory of Open Quantum Systems, (Oxford University Press, USA, 2010).
- 3. Gibbons, K. S., Hoffman, M.J., Wootters, W. K., Discrete phase space based on finite fields. Phys. Rev A 70, 062101 (2004).
- 4. Galvão, E. F., Discrete Wigner functions and quantum computational speedup. Phys. Rev A 71, 042302 (2005).
- 5. Casaccino, A., Galvão, E. F., Severini, S., Extrema of discrete Wigner functions and application. Phys. Rev A 78, 022310 (2008).
- 6. Dam, W., Howard, M., Noise thresholds for higher-dimensional systems using the discrete Wigner function. Phys. Rev A 83, 032310 (2011).

Thank you jai.1@iitj.ac.in

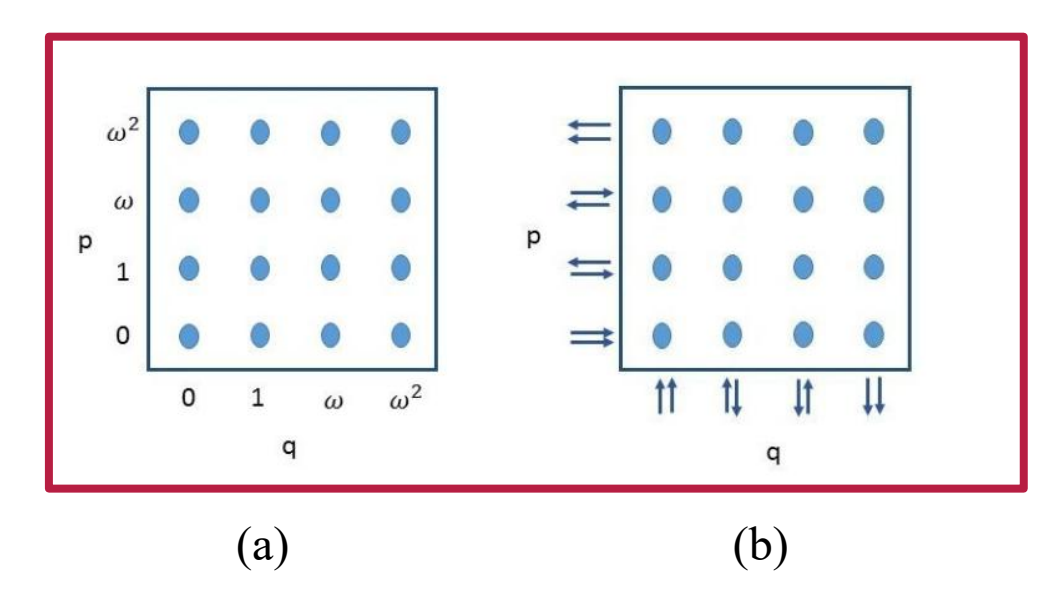


Ingredients required to define a class of discrete Wigner functions:



Discrete phase space

- For a system defined in a Hilbert space of power of prime dimension d, the discrete phase space is an array of $d \times d$ points.
- The horizontal and the vertical axes of the discrete phase space are associated with two non-commuting observables.
- Points in the discrete phase space are labeled by the elements of the Galois field F_d .
- A "line" is a set of d points in discrete phase space.
- For fixed values of a and b when c is varied over F_d in the equation aq + bp = c, a set of d parallel lines known as a **striation** is generated.



- (a) Labeling the points of 4×4 phase space by a finite field.
- (b) Labeling the lines of the discrete phase space with pure states.

Ingredients required to define a class of discrete Wigner functions:



- For prime power dimensions, there are (d + 1) striations in the discrete phase space, and (d + 1) Mutually unbiased bases (MUB's).
- Each striation contains d lines analogously each MUB contains d basis vectors.

We denote each line by $\lambda_{i,j}$, *i.e.*, the j-th line of the i-th striation and $|\alpha_{i,j}\rangle$ is the j-th vector of the i-th MUB.

Mutually Unbiased Bases (MUB's)

Two different orthonormal bases B_1 and B_2 :

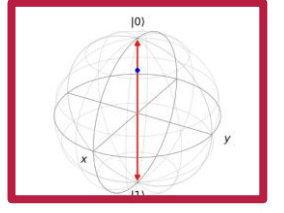
$$B_1 = \{ |\alpha_{1,1}\rangle, |\alpha_{1,2}\rangle, \dots, |\alpha_{1,d}\rangle\}, |\langle \alpha_{1,i}|\alpha_{1,j}\rangle|^2 = \delta_{i,j},$$

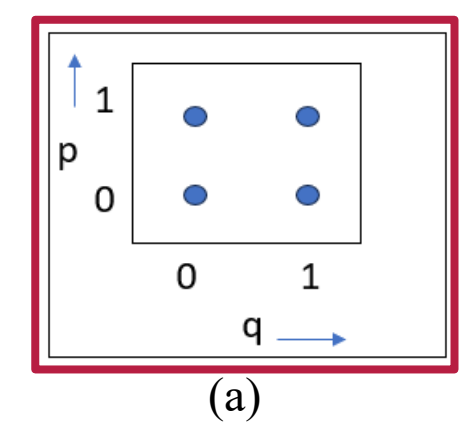
$$\mathbf{B}_2 = \{ |\alpha_{2,1}\rangle, |\alpha_{2,2}\rangle, \dots, |\alpha_{2,d}\rangle\}, |\langle\alpha_{2,i}|\alpha_{2,j}\rangle|^2 = \delta_{i,j},$$

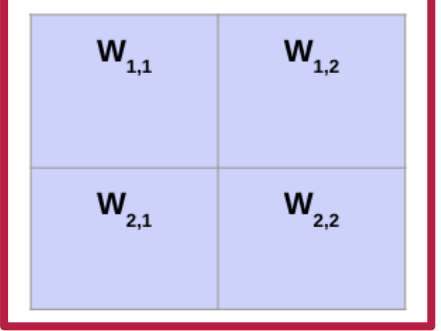
are said to be mutually unbiased or mutually conjugate if

$$\left|\left\langle \alpha_{i,j} \left| \alpha_{k,l} \right\rangle \right|^2 = \frac{1}{d}$$
 if $i \neq k$.

DWFs: Single-qubit systems

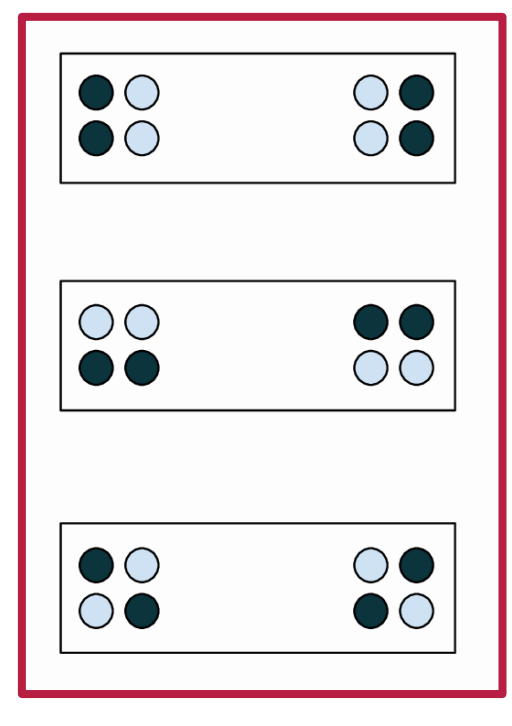






(b)

- (a) Labeling of the points of 2×2 phase space by a finite field F_2 .
- (b) Labeling of the points of 2×2 phase space by discrete Wigner function elements.



Lines and striations of the 2×2 phase space

Striation	MUBs associated with striation
1	$\binom{0}{1}$, $\binom{1}{0}$
2	$\frac{1}{\sqrt{2}}\binom{1}{1}, \frac{1}{\sqrt{2}}\binom{1}{-1}$
3	$\frac{1}{\sqrt{2}} \binom{1}{i}, \frac{1}{\sqrt{2}} \binom{1}{-i}$

The MUBs associated with lines of the 2×2 discrete phase space of single-qubit systems.

$$\mathbf{W}_{1,1} + \mathbf{W}_{2,1} = p_{1,1} , \qquad (1)$$

$$\mathbf{W}_{1,2} + \mathbf{W}_{2,2} = p_{1,2} , \qquad (2)$$

$$\mathbf{W}_{2,1} + \mathbf{W}_{2,2} = p_{2,1} , \qquad (3)$$

$$\mathbf{W}_{1,1} + \mathbf{W}_{1,2} = p_{2,2} , \qquad (4)$$

$$\mathbf{W}_{1,1} + \mathbf{W}_{2,2} = p_{3,1} , \qquad (5)$$

$$\mathbf{W}_{1,2} + \mathbf{W}_{2,1} = p_{3,2} . \qquad (6)$$

$$\mathbf{W}_{1,2} + \mathbf{W}_{2,1} = p_{3,2} . \qquad (6)$$

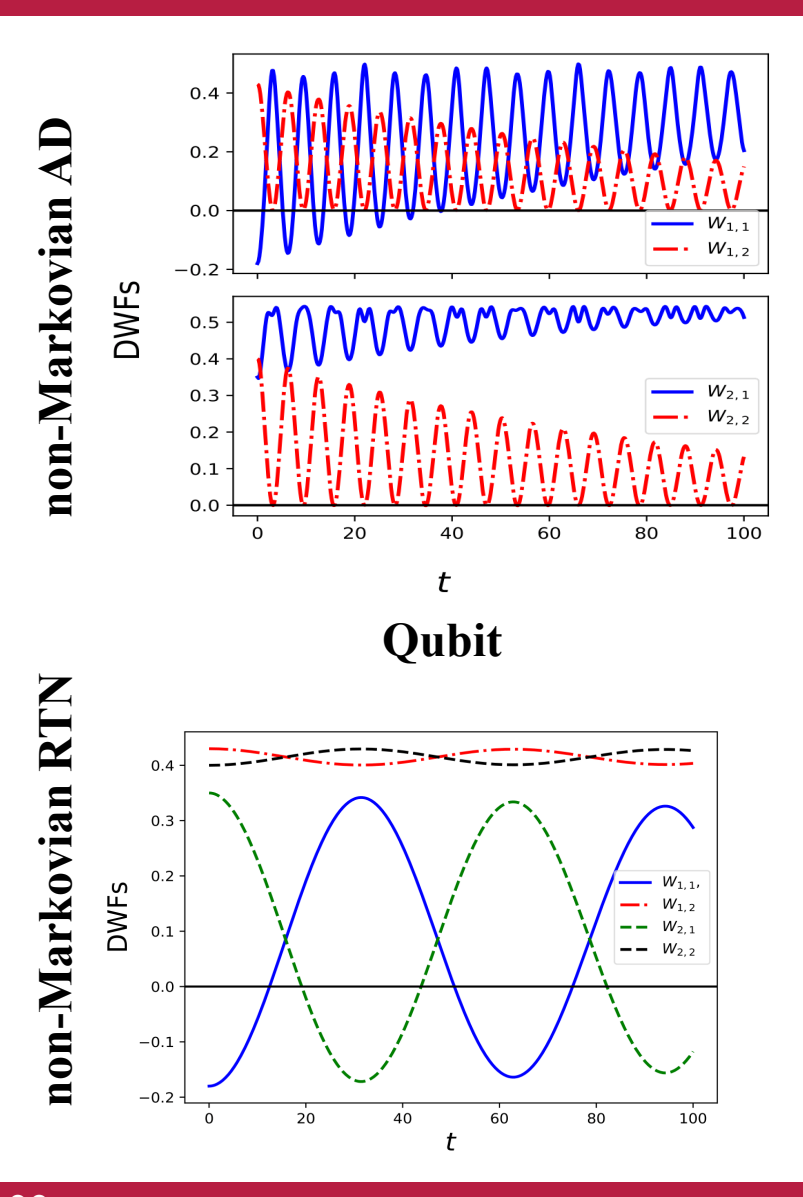
Noisy quantum channels:

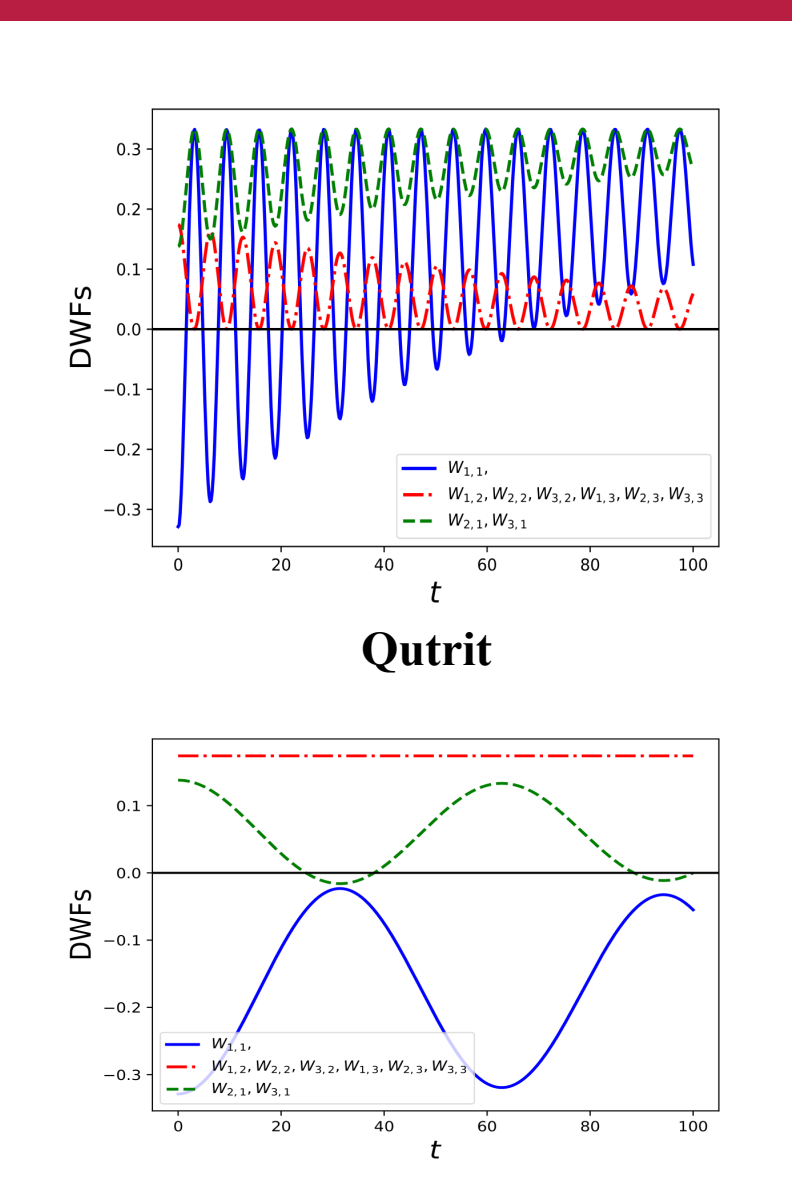


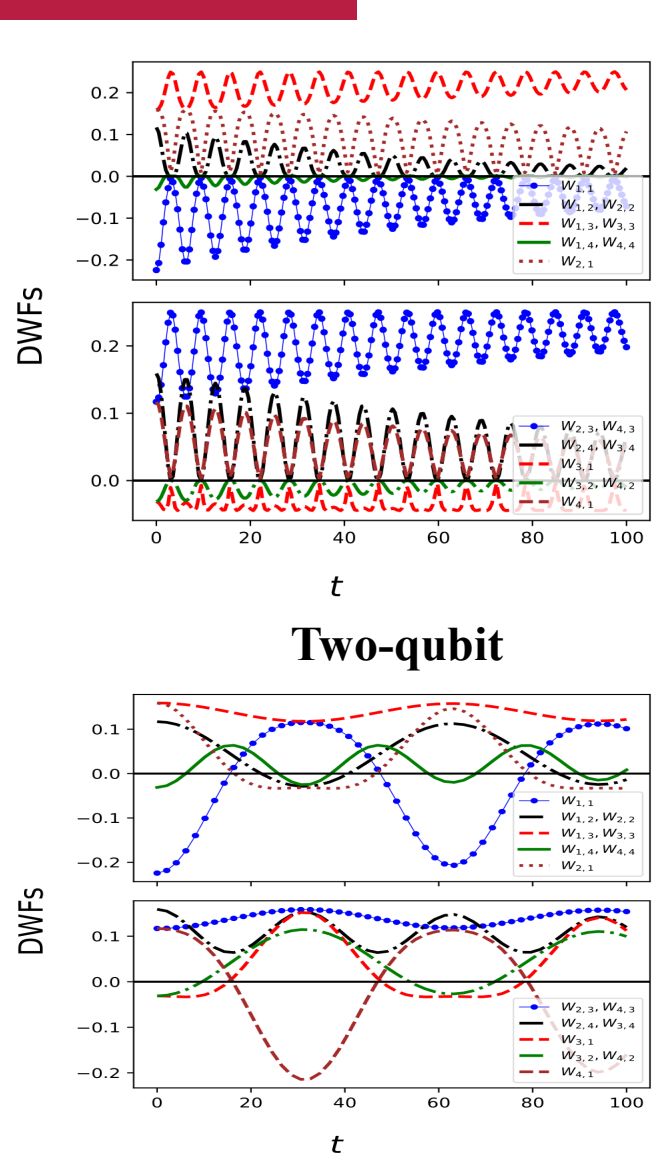
Noise	Kraus operators	Noise function
(non)-Markovian AD	$K_0^{AD} = \begin{bmatrix} 1 & 0 \\ 0 & \sqrt{1 - \lambda(t)} \end{bmatrix}$	$\lambda(t) = 1 - e^{-gt} \left(\frac{g}{l} \sinh\left(\frac{lt}{2}\right) + \cosh\left(\frac{lt}{2}\right) \right)^2$
	$K_1^{AD} = \begin{bmatrix} 0 & \sqrt{\lambda(t)} \\ 0 & 0 \end{bmatrix}$	$l = \sqrt{g^2 - 2\gamma g}$
(non)-Markovian RTN	$K_0^{RTN} = \frac{\sqrt{1 + \Lambda(t)}}{2} I_2$	$\Lambda(t) = e^{-\gamma t} \left(\cos(\zeta \gamma t) + \frac{\sin(\zeta \gamma t)}{\zeta} \right)$
	$K_1^{RTN} = \frac{\sqrt{1 - \Lambda(t)}}{2} \sigma_z$	$\zeta = \sqrt{\left(\frac{2b}{\gamma}\right)^2 - 1}$

Results: discrete Wigner functions



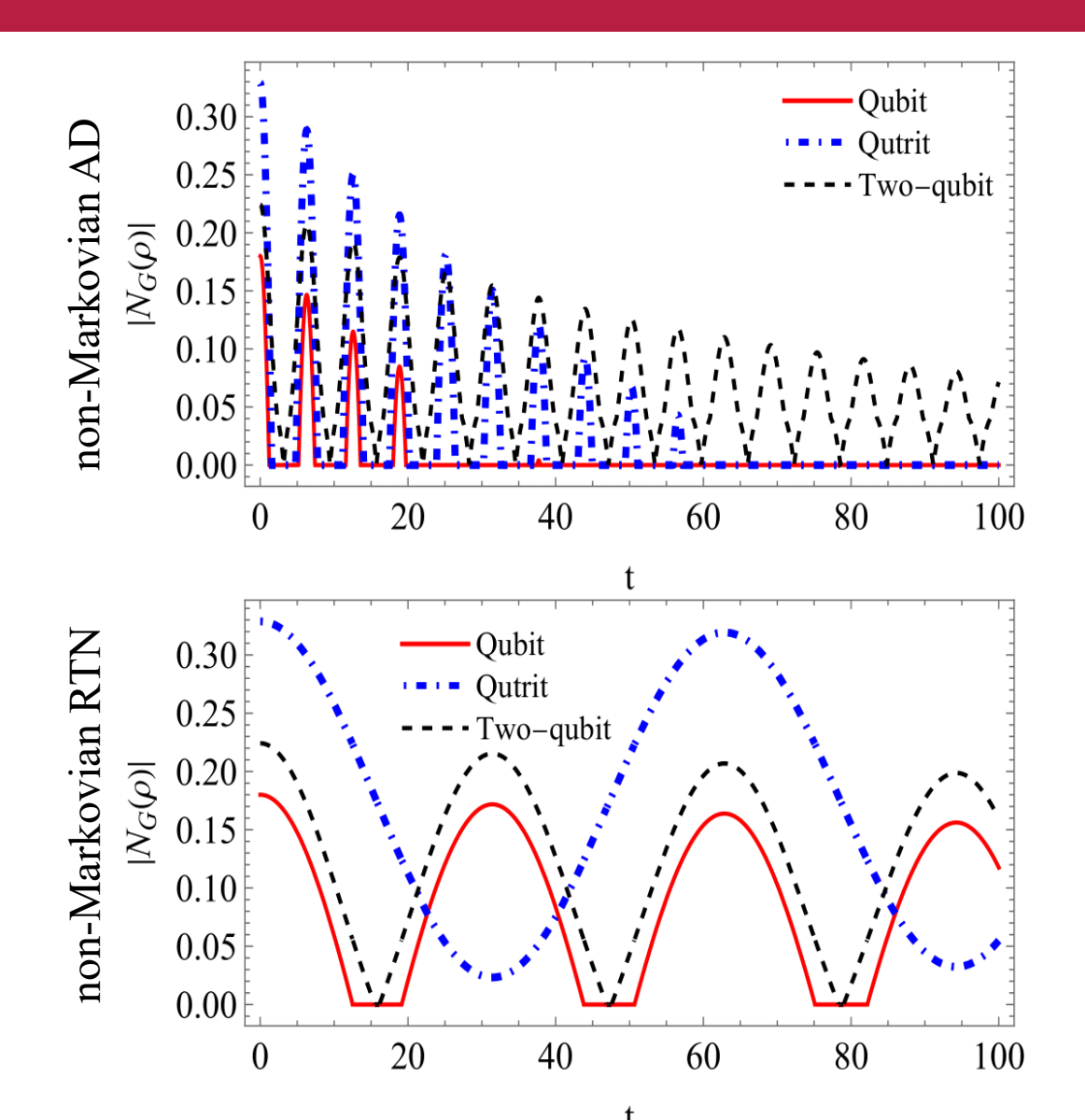






Results: discrete Wigner negativity

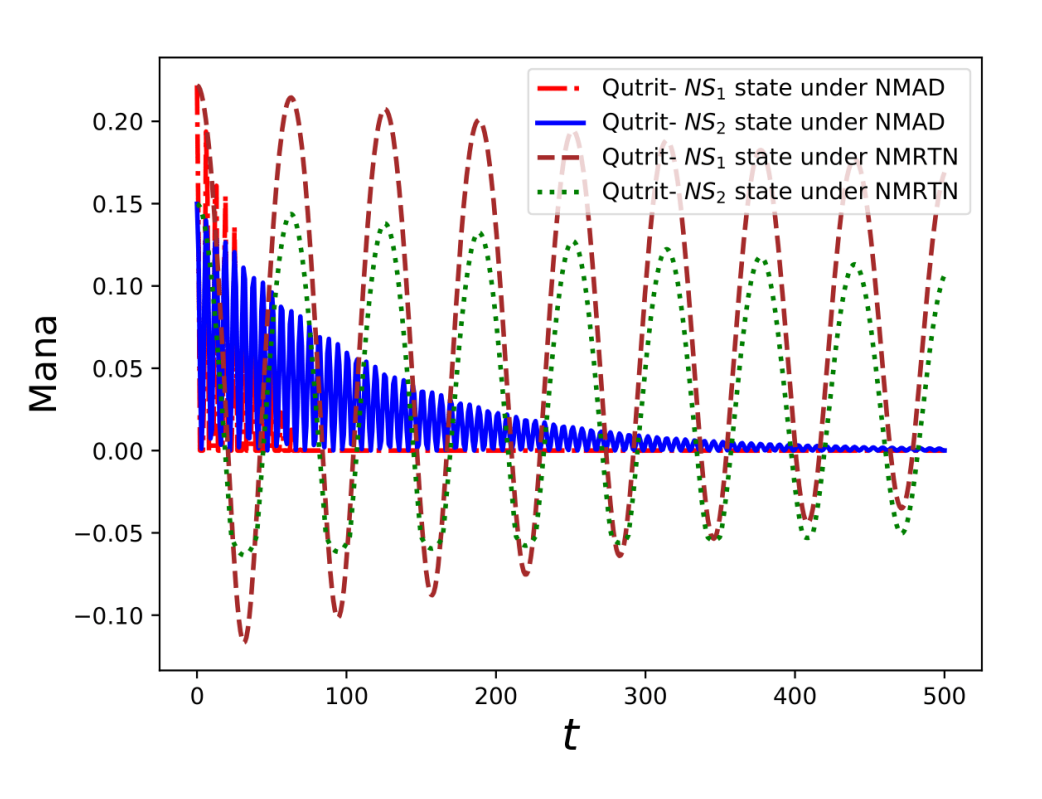




- \triangleright It is highest for odd prime dimension, *i.e.*, qutrit NS_1 state compared to qubit and two-qubit NS_1 state.
- \triangleright Under the influence of (non)-Markovian AD noise, the two-qubit NS_1 state sustains for a longer duration than the single qubit and qutrit NS_1 state.
- \triangleright Under non-Markovian RTN, all the cases , i.e., qubit, qutrit, two-qubit, NS_1 state show expected oscillatory behavior, with the peaks and dips of qubit and two-qubit in synchronization, with an alternate pattern with the qutrit.

Results: Mana

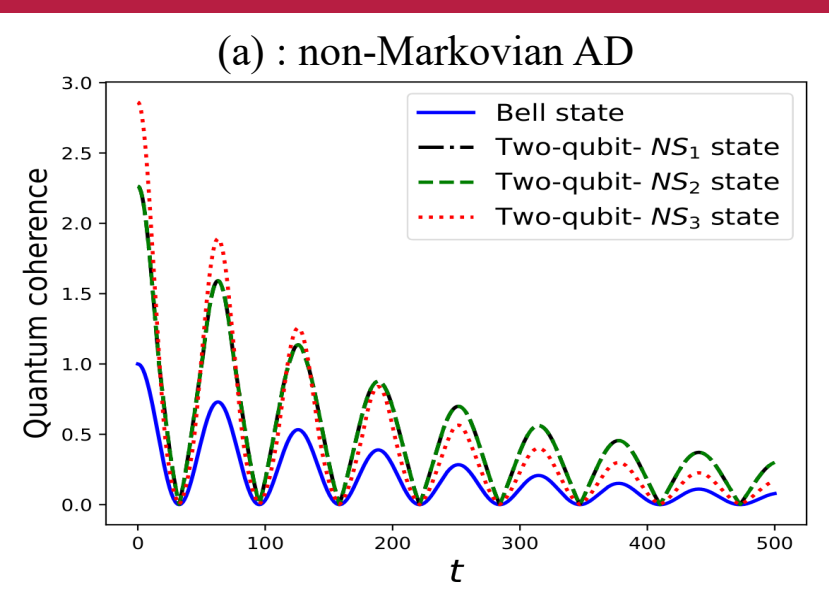


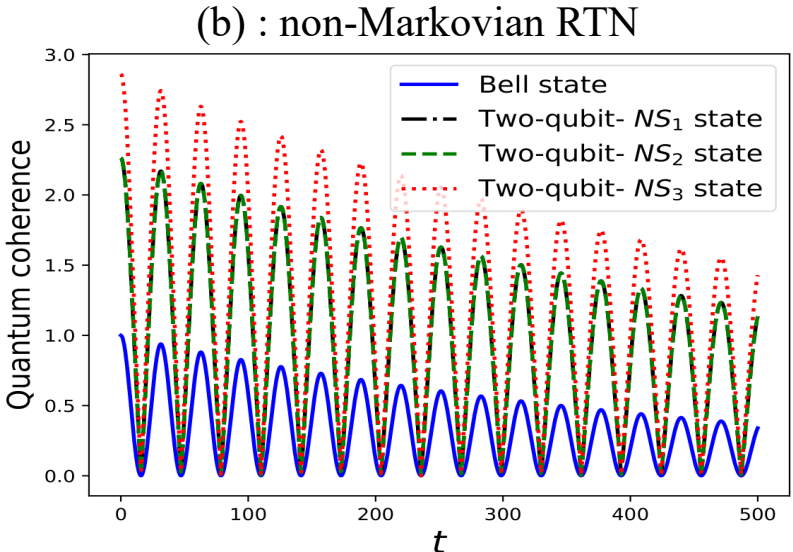


- Initially, the NS_1 state has a higher value of mana than the NS_2 state. However, it dies off very quickly in comparison to the NS_2 state. Hence, the NS_2 state persists longer and has a finite mana value in presence of non-Markovian AD noise.
- ➤ Under the non-Markovian RTN, mana for both the negative quantum states of qutrit show expected oscillatory behavior which is persistent for much longer than the non-Markovian AD

Results: Coherence





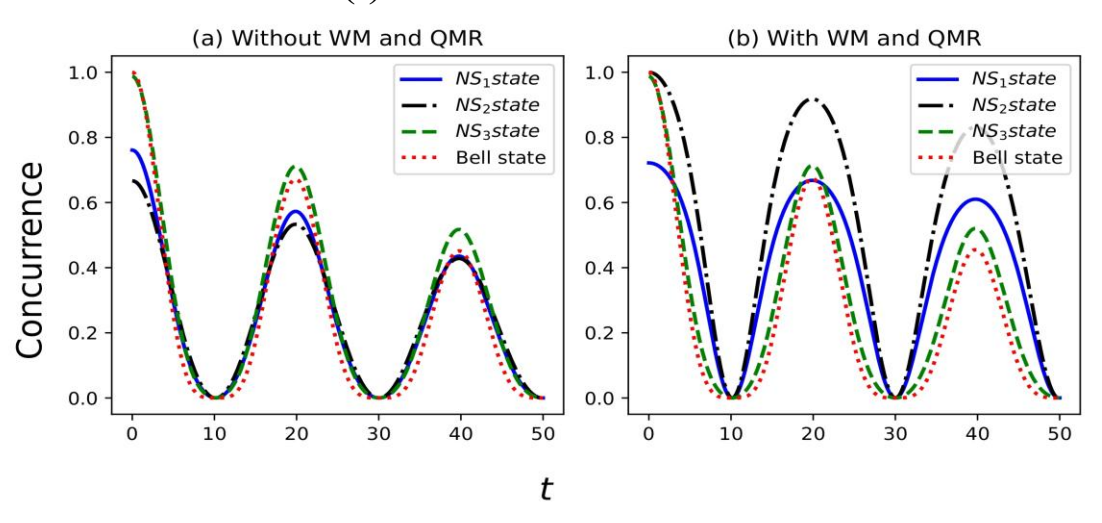


- Two-qubit negative quantum states have quantum coherence greater than the Bell state. Also among the negative quantum states the NS_3 state dominates all others at t = 0.
- All the states display anticipated decaying oscillatory behavior under the non-Markovian AD and RTN channel.
- For long duration under non-Markovian AD the NS_1 and NS_2 states coherence is higher then the NS_3 and Bell states.
- The NS_3 state's coherence is higher than all other considered states under non-Markovian RTN channel.

Results: Concurrence

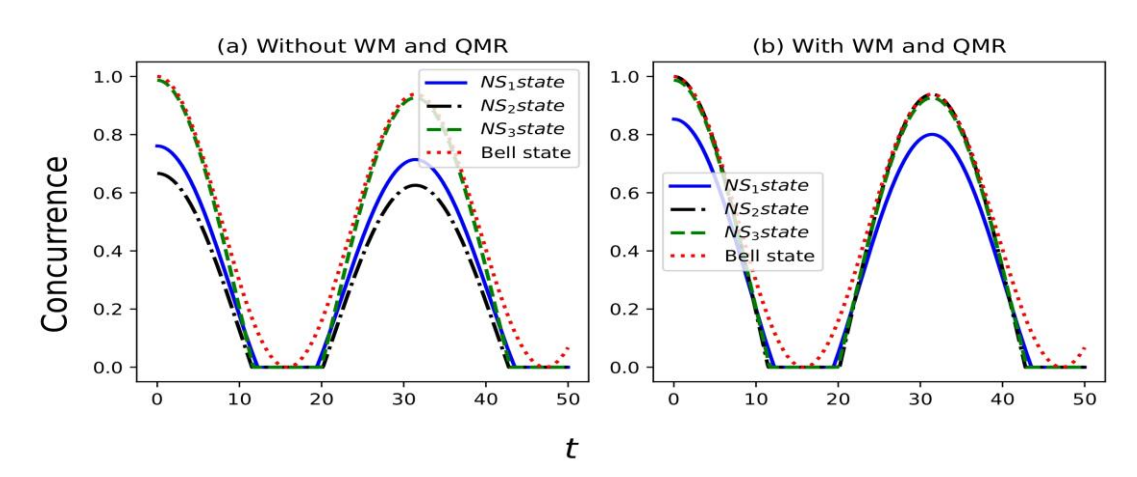


(i) non-Markovian AD



- For a longer duration, the $|NS_3\rangle$ state dominates the Bell state and other two-qubit negative quantum states.
- ➤ With WM and QMR, the two-qubit negative quantum states dominate the Bell state in terms of preserving their entanglement under non-Markovian AD noise for a longer duration.

(ii) non-Markovian RTN

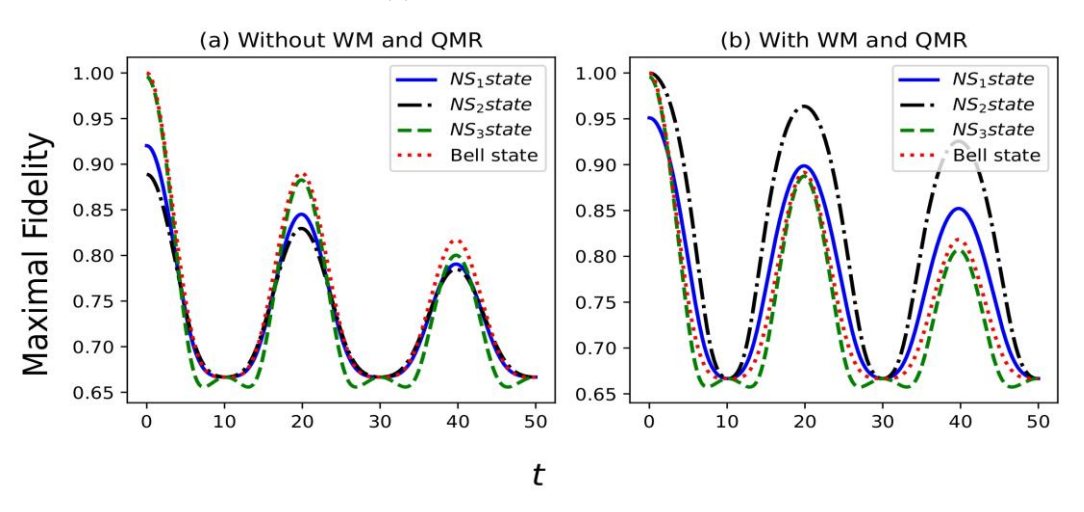


- Under non-Markovian RTN channel the $|NS_3\rangle$ state shows entanglement variations almost equal to the Bell state, and both have the highest entanglement over time.
- The $|NS_2\rangle$ state exhibits entanglement comparable to that of the Bell state and $|NS_3\rangle$ state over time when WM and QMR are employed.

Results: Maximal fidelity

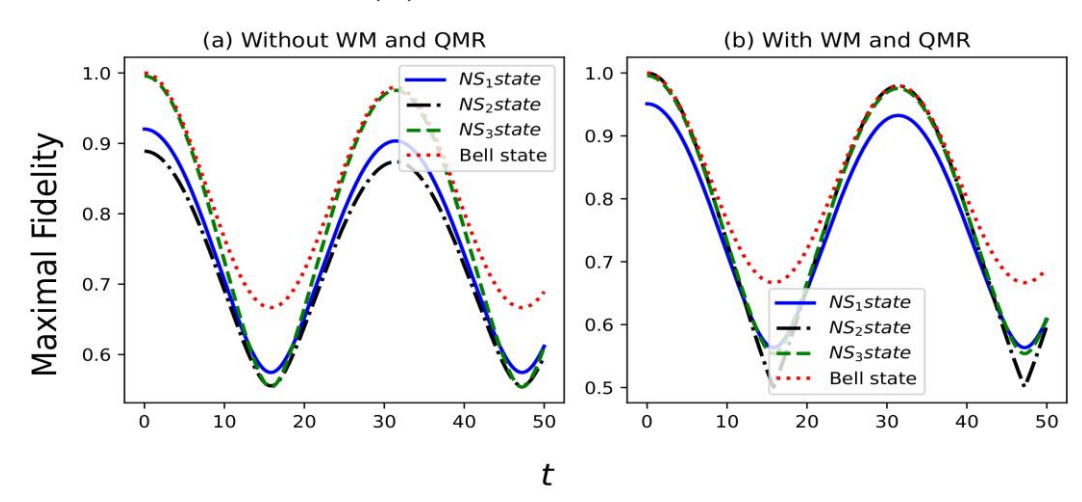


(i) non-Markovian AD



- > Just like the Bell state, all the considered two-qubit negative quantum states have maximal fidelity always greater than 2/3.
- The $|NS_1\rangle$ and $|NS_2\rangle$ state's fidelity leads the Bell state with WM and QMR.

(ii) non-Markovian RTN

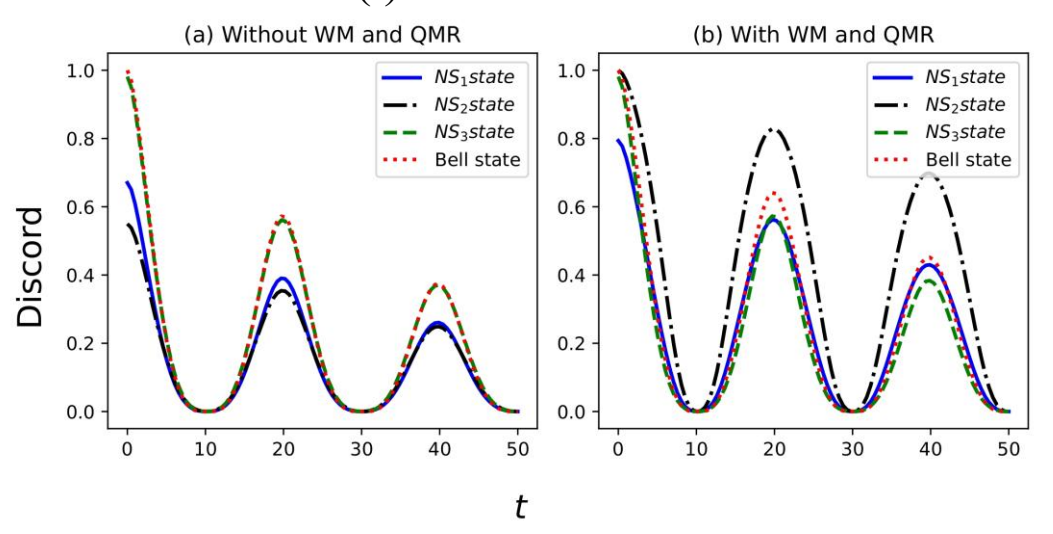


- ➤ The decay in maximal fidelity over time of all the considered states is gradual compared to the non-Markovian AD noise.
- With WM and QMR, the $|NS_2\rangle$ state's maximal fidelity variations are comparable to the $|NS_3\rangle$ state.

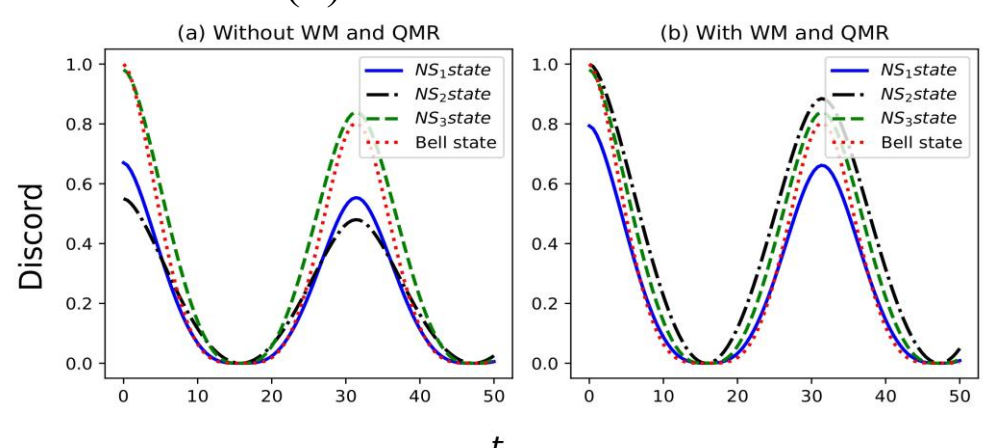
Results: Discord



(i): non-Markovian AD



(ii): non-Markovian RTN



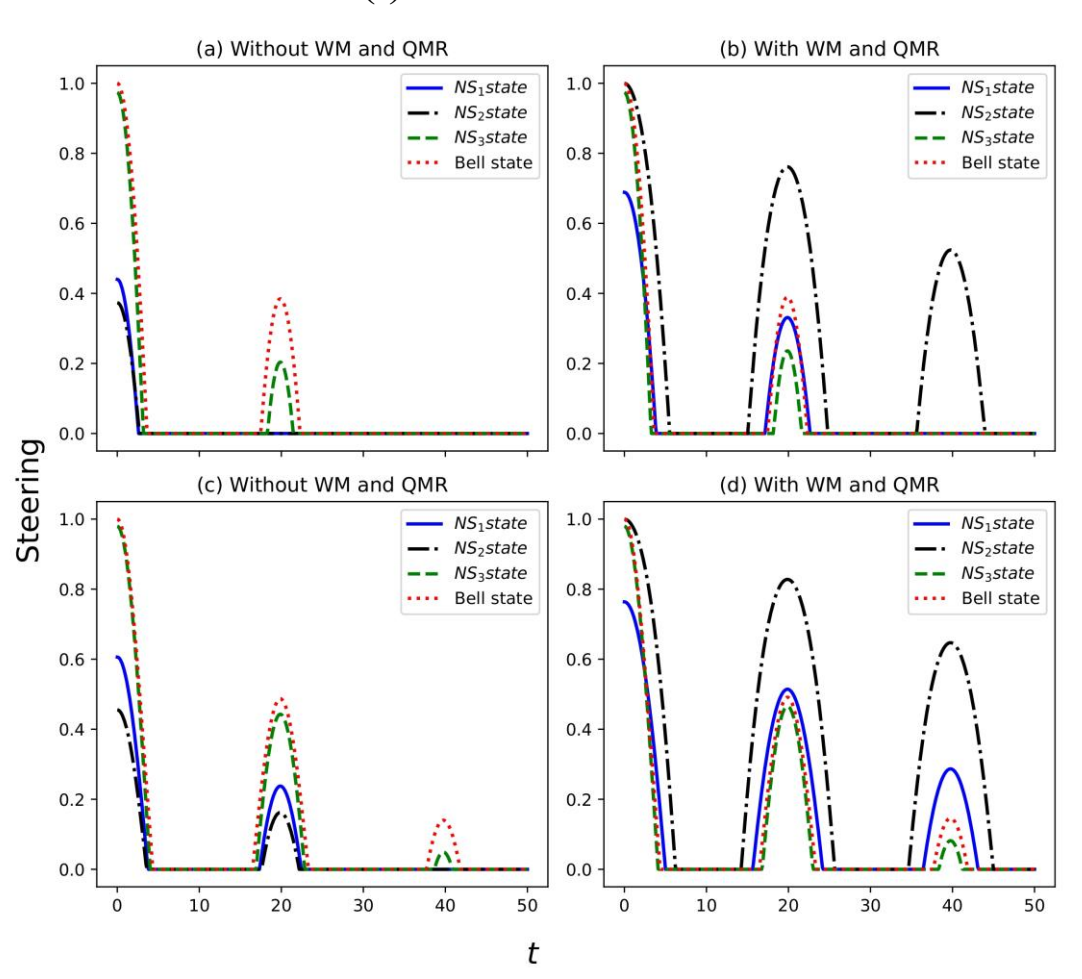
- \triangleright The variation of discord of NS_3 state is similar to the Bell state and these states have the highest discord under non-Markovian AD noise.
- The discord of the NS_1 and NS_2 states can be seen to be enhanced by the WM and QMR. In fact, the NS_2 state shows more discord over time than all other considered states.

- ➤ The *NS*₃ state discord dominates the Bell state and other considered states over time under the non-Markovian RTN channel.
- With WM and QMR, at t = 0, the NS_2 state shows discord equal to the Bell state and NS_3 state. It also dominates all other considered states over time.

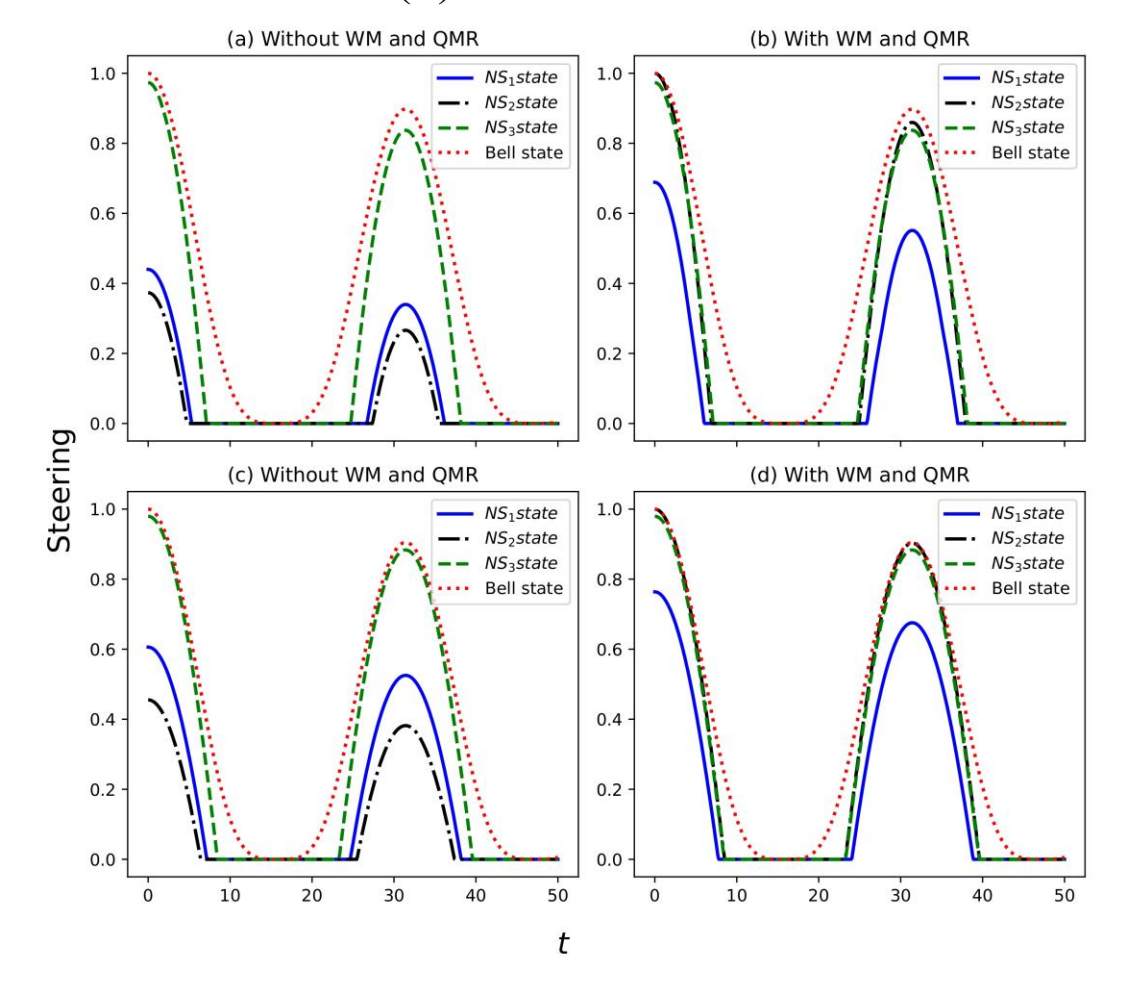
Results: Steering



(i): non-Markovian AD



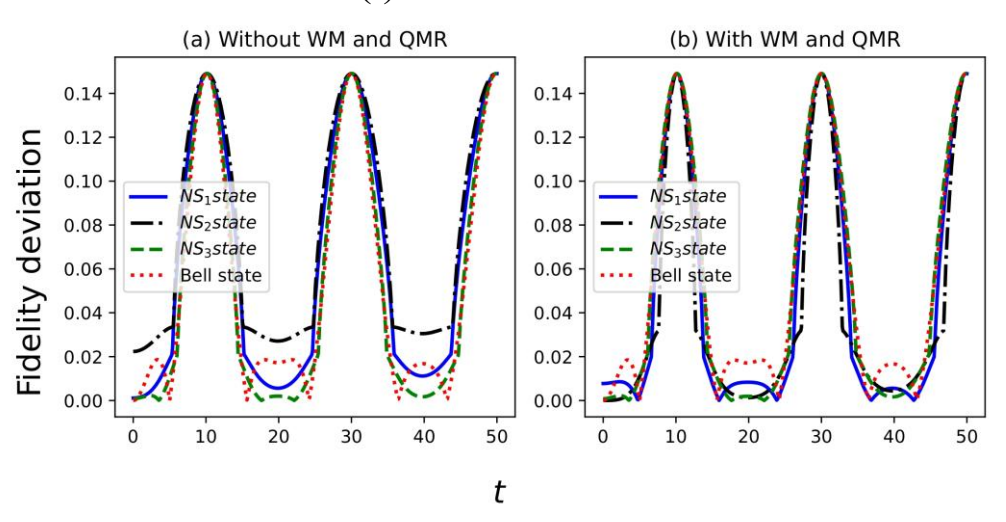
(ii): non-Markovian RTN



Results: Fidelity deviation

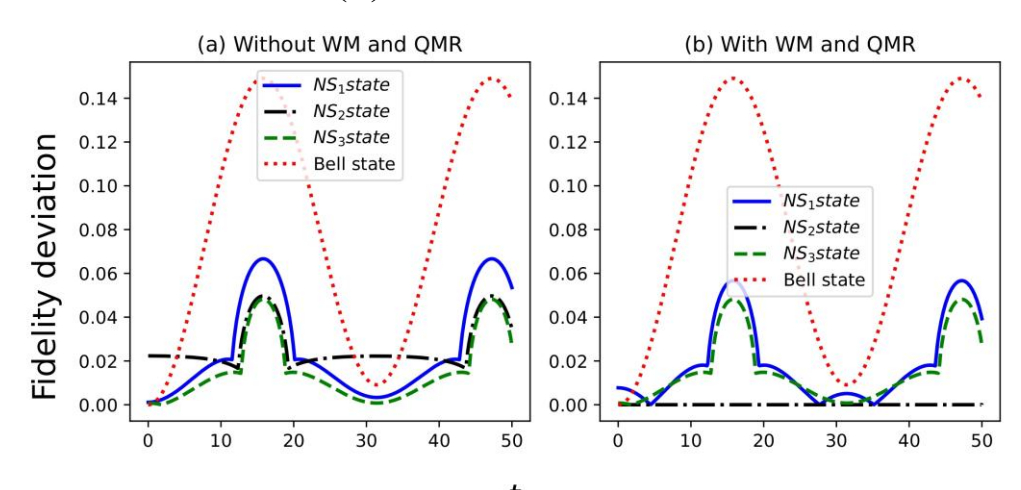


(i) non-Markovian AD



- \triangleright The $|NS_3\rangle$ state is relatively better among all considered quantum states for universal quantum teleportation (UQT).
- The WM and QMR squeeze the non-zero fidelity deviation area of $|NS_1\rangle$ and $|NS_2\rangle$ states in contrast to the $|NS_3\rangle$ and Bell states.

(ii) non-Markovian RTN



- All the two-qubit negative quantum states show less fidelity deviation than the Bell state.
- With the WM and QMR, the $|NS_2\rangle$ state shows zero deviation in fidelity under the non-Markovian RTN channel, making it an ideal state for UQT.